Flaw Stability in Mild Steel Tanks in the Upper-Shelf Ductile Range - Part II: J-Integral Based Fracture Analysis

Poh-Sang Lam and Robert L. Sindelar

Savannah River Technology Center
Westinghouse Savannah River Company
Aiken, South Carolina 29808

This document was prepared in conjunction with work accomplished under Contract No. DE-AC09-96SR18500 with the U. S. Department of Energy.

Abstract

The J-integral fracture methodology was applied to evaluate the stability of postulated flaws in mild steel storage tanks. The material properties and the J-resistance (J_R) curve were obtained from the archival A285 Grade B carbon steel test data. The J-integral calculation is based on the center-cracked panel (CCP) solution of Shih and Hutchinson (1976). A curvature correction was applied to account for the cylindrical shell configuration. A finite element analysis of an arbitrary flaw in the storage tank demonstrated that the curvature-corrected CCP solution is a close approximation. The maximum storage tank fluid level for a postulated flaw size can be established based on the J-integral flaw stability methodology.

Introduction

Mild steel storage tanks are widely used in the petrochemical and nuclear industry. The A285 Grade B carbon steel is one of the commonly used materials of construction in such tanks. A key element in assessing the fitness-for-service of aged mild steel storage tanks is the flaw stability analysis. In applications where the normal operating temperature of the tanks is 70°F (21°C) and above, A285 Grade B carbon steel falls in the upper transition region where ductile fracture would be the failure mode. The fracture mechanics methodology that best describes material behavior to evaluate flaw stability in such structures is the J-integral based elastic-plastic analysis in which stable tearing is taken into consideration. This paper presents the J-T flaw stability methodology and the results of the analyses, where T denotes the tearing modulus.

The analyses require materials property inputs for A285 carbon steel. Tensile and fracture properties, including the effect of age-related degradation, have been assimilated and discussed by Sindelar, Lam, Caskey, and Woo (1999). The flaw stability evaluation for the mild steel storage tank presented in this paper uses the lower bound J_R curve from the above referenced paper. This lower bound curve is considered to provide a conservative analysis when applied to tanks where the minimum operating temperature of 70°F (21°C) is higher than the mechanical property test temperature of 40°F (4.4°C). Both temperatures are within the regime where crack extension is stable, crack advance proceeds by ductile tearing, and where toughness or resistance to ductile crack propagation increases as the temperature rises. Therefore, fracture resistance at the tank operating temperature would be greater than that obtained at 40°F (4.4°C).

The analytical solution for a center-cracked panel developed by Shih and Hutchinson (1976) was primarily used to evaluate the J-integral values under applied load. A curvature correction procedure developed by Lam, Sindelar, and Awadalla (1993) was used to account for the tank geometry. The stress intensity factor due to residual stress was also included.

The J-integral value at which flaw instability occurs was taken from the lower bound specimen data for J_R curve when the crack extension reached 1.5 mm (0.06 inches), the termination point of the test data, and was well within the stable growth regime. The instability crack length corresponding to this critical J value versus applied load can therefore be obtained.

A finite element analysis for an arbitrary flaw in a storage tank has been performed. The analysis demonstrated that the center-cracked panel solution is a close approximation for the flaw stability analysis of this type of mild steel storage tanks. An example is used to illustrate the development of a maximum storage tank fluid level as a function of the fluid density for various crack sizes in highly stressed region of the tank.

J-T Flaw Stability Methodology

J-T Analysis of Flaw Stability

The tearing stability of the material is characterized by the tearing modulus (T), which is defined by

$$T = \frac{E}{\sigma_o^2}\frac{dJ}{da}$$

where J is the value of J-integral, σ_o is the 0.2% yield stress, E is the Young's modulus, and da is an incremental crack extension. Instability flaw lengths are evaluated based on the loading conditions of the structural component and are determined by an elastic-plastic J-integral or J-T analysis. The crack growth ($J \geq J_{IC}$) is stable if $T < T_R$, where T_R is the tearing modulus of the material. As schematically shown in Figure 1, the intersection point of the applied J-T curve and the material J-T curve will determine the crack growth stability limit.

Development of Material J-T for Flaw Stability Analysis

The J_R curves were developed from the 0.4C(T) fracture toughness tests of the A285 (Sindelar et al., 1999). A lower bound J_R curve for A285 compact tension specimen tests is shown in Figure 2. The material J_R curve was obtained from a power law fit to the experimental data:

$$J = C(\Delta a)^m$$

where Δa is the crack extension. The material parameters C and m are determined through curve fitting. For this lower bound curve in Figure 2, C= 328.1 N/(mm)$^{m+1}$ and m= 0.6578. It should be noted that the last data point represents the termination of the compact tension test, rather than the rupture failure of the specimen. The power law formulation of the $J(\Delta a)$ obtained from material testing can be plotted with its tearing modulus, $T(\Delta a)$, to produce the material J-T curve.

Determination of J-Δa Cut-off for J-controlled Growth in C(T) Specimens

Stable crack growth occurs under conditions where additional deformation is needed to maintain the appropriate level of strain concentration at the crack tip (Hutchinson and Paris, 1979). The J-integral is an appropriate parameter for characterizing crack growth provided increments in the strain field that are proportional to applied load are greater than increments which are nonproportional to the applied load. These conditions may be expressed as,

$(dJ/da)(b/J) \equiv \omega >> 1$, where b is the uncracked ligament size.

Crack extension in C(T) specimens generally limits (in ASTM standards E399, E813, and E1152) the region of the plastically blunted crack tip in relation to the in-plane dimension of the specimen (remaining ligament). Tough materials (large J value) such as austenitic stainless steels or carbon steels do not generally meet the criteria when tested above the nil-ductility transition temperature (NDTT) for small planforms. Data at high crack extension from these specimens can be applied in elastic-plastic fracture analyses if J-controlled growth can be established.

A program to measure the fracture toughness of austenitic stainless steel was completed in the early 1990s. Test results from the program can be applied to evaluate J-controlled growth in the 0.394T planform specimens for the carbon steel test program since both materials have similar yield strengths of approximately 35 ksi or 240 MPa. The measurement of an austenitic stainless steel specimen in both the large planform (0.394×1T, the width of the specimen is 2 inches or 50.8 mm measured from the load line to the back face of the specimen) and small planform (0.394T, the width of the specimen is 0.788

inches or 20.0 mm measured from the load line to the back face of the specimen) allows a direct comparison of J-deformation versus crack extension (Fig. 3). Deviation of the small specimen J_R curve from the large specimen curve would indicate the point (Δa) at which the toughness (defined by the deformation theory) is changing due to size effects. Figure 3 shows that the J values from the small planform deviate markedly from the large planform values at crack extensions greater than 3 mm (0.12 inches). Above this point, the J values from the small planform specimen are lower (conservative) compared to the large planform results. The point of deviation between the large and small planform results is suggested to indicate the limit of validity of J-deformation for the 0.394T planform specimen. For the lower bound carbon steel specimen (Fig. 2), the value of the ω factor is 1.5 at 3-mm (0.12-inch) crack extension for this 0.394T planform. Note that the value of ω is significantly less than the proposed value ($\omega >> 1$).

In some applications including the present case, the material J-T curve does not intersect with the applied J-T curve, unless the material J-T curve is extrapolated extensively. Under these circumstances, a cut-off J value is conservatively used (rather than extrapolation) to determine the instability crack length. Therefore, in the current flaw stability analysis, a cut-off J-integral value as shown in Figure 2 is taken as 450 kJ/m^2 (2570 in-lb/in^2) which corresponds to a crack extension at about 1.5 mm (0.06 inches) in a 0.394T planform (Sindelar et al., 1999).

Center-Cracked Panel Solution (Shih and Hutchinson, 1976)

The Ramberg-Osgood power law for stress and strain can be expressed as

$$\frac{\varepsilon}{\varepsilon_o} = \frac{\sigma}{\sigma_o} + \alpha\left(\frac{\sigma}{\sigma_o}\right)^n,$$

where σ_o is the 0.2% yield stress and ε_o is the corresponding elastic strain. Figure 4 shows a uniaxial tension test result for a specimen representing a material property lower bound based on its J_R curve and J_{IC} value (Fig. 2). The true stress-true strain curve is characterized with α=17.176 and n= 3.585 (Sindelar, et al., 1999).

A solution of J-integral for a center-cracked panel (CCP) with a finite width (2b) under plane stress condition for Ramberg-Osgood materials was obtained by Shih and Hutchinson (1976):

$$\frac{J}{\sigma_o \varepsilon_o a(1-a/b)} = \psi \left(\frac{P}{P_o}\right)^2 g_1\left(\frac{a_{eff}}{b}, n=1\right) + \alpha\left(\frac{P}{P_o}\right)^{n+1} g_1\left(\frac{a_{eff}}{b}, n\right).$$

Note that the total J-integral can be composed of two parts, the elastic portion (J_{el}^{ccp}) and a plastic portion (J_{pl}^{ccp}). Therefore,

$$J_{el}^{ccp} = \psi\, \sigma_o \varepsilon_o\, a(1-a/b)\left(\frac{P}{P_o}\right)^2 g_1\left(\frac{a_{eff}}{b}, n=1\right)$$

$$J_{pl}^{ccp} = \alpha\, \sigma_o \varepsilon_o\, a(1-a/b)\left(\frac{P}{P_o}\right)^{n+1} g_1\left(\frac{a_{eff}}{b}, n\right),$$

where a is the half crack length, b is the half specimen width, $\varepsilon_o = \sigma_o / E$,

$a_{eff} = a + \varphi r_y$, $P \le P_o$ (Kumar and Shih, 1980),

$a_{eff} = (a_{eff})_{P=P_o}$, $P > P_o$,

$\varphi = \dfrac{1}{1 + (P/P_o)^2}$,

$P_o = 2(b-a)\sigma_o$ is the lower bound limit load,

$P = 2b\sigma^{\infty}$ is the applied load corresponding to a remote stress σ^{∞},

$r_y = \dfrac{1}{2\pi}\left(\dfrac{n-1}{n+1}\right)\left(\dfrac{K_I}{\sigma_o}\right)^2 = \dfrac{a}{2\pi}\left(\dfrac{n-1}{n+1}\right)\left(1 - \dfrac{a}{b}\right)\left(\dfrac{P}{P_o}\right)^2 g_1\left(\dfrac{a}{b}, 1\right)$ for plane stress,

$\psi = \dfrac{a_{eff}}{a}\left(\dfrac{b-a}{b-a_{eff}}\right)$,

and

$$g_1\left(\frac{a}{b},1\right) = \pi\left[1 - 0.5\frac{a}{b} - 0.37\left(\frac{a}{b}\right)^2 - 0.044\left(\frac{a}{b}\right)^3\right]^2$$

For this material, the values for g_1(a/b, n=3.585) can be calculated according the procedure outlined in Shih and Hutchinson (1976):

a/b	g_1(a/b, n=3.585)
0	6.133
1/8	4.152
1/4	3.156
1/2	1.984
3/4	1.385
1	0.916

A simpler solution for an infinite plate can also be found in Shih and Hutchinson (1976). That solution is also valid for this type of large tank geometry (the radius to thickness ratio is greater than 800).

Curvature Correction

This analytic solution (J^{ccp}) provides a basis for constructing an approximate solution (J^{cur}) for the sidewall of a storage tank by the application of a curvature correction factor (Lam, Sindelar, and Awadalla, 1993). The correction factors (Y) can be derived from a linear elastic stress intensity factor (K) solution of Tada, Paris, and Irwin (1973). Assumptions have been made: 1) The correction factor for J-integral is Y^2 since elastic J-integral is proportional to K^2; and 2) Same correction factor is applied to the elastic portion of J-integral as well as to its plastic portion ($J_{el}^{cur} = Y^2 J_{el}^{ccp}$ and $J_{pl}^{cur} = Y^2 J_{pl}^{ccp}$).

For an axial flaw opened by hoop stress (σ_H), the stress intensity factor for a crack with length 2a in a cylinder with mean radius R and thickness t is (Tada, et al. 1973)

$K_I = \sigma_H\sqrt{\pi a}\, Y_1(\lambda)$, where $\lambda = \dfrac{a}{\sqrt{Rt}}$. Therefore, the correction factor for an axial crack is

$$Y_1(\lambda) = \sqrt{1 + 1.25\ \lambda^2} \quad \text{for} \quad 0 < \lambda \le 1, \text{ or}$$
$$Y_1(\lambda) = 0.6 + 0.9\ \lambda, \quad \text{for} \quad 1 \le \lambda \le 5.$$

For a circumferential crack with length 2a or angle 2θ subjected to a longitudinal stress σ_L, the stress intensity factors are (Tada et al. 1973)

$$K_I = \sigma_L \sqrt{\pi a}\ Y_2(\lambda \text{ or } \theta),$$

where

$$Y_2(\lambda) = \sqrt{1 + 0.3225\ \lambda^2} \quad \text{for} \quad 0 < \lambda \le 1,$$

$$Y_2(\lambda) = 0.9 + 0.25\ \lambda, \quad \text{for} \quad 1 \le \lambda \le 5,$$

and

$$Y_2(\theta) = \sqrt{\frac{2}{\eta}\frac{1}{\pi\theta}}\ f(\theta), \quad \text{for} \quad \lambda > 5,$$

in which

$$\eta^2 = \frac{t / R}{\sqrt{12\left(1 - \nu^2\right)}}$$

and

$$f(\theta) = \theta + \frac{1 - \theta\ \cot\theta}{2\ \cot\theta + \sqrt{2}\ \cot\left(\frac{\pi - \theta}{\sqrt{2}}\right)}$$

Procedure of Combining J-integral Solutions

(1) For a given applied remote stress, calculate the CCP solution of Shih and Hutchinson for various crack lengths. The J-integral (J^{ccp}) is composed of an elastic portion (J_{el}^{ccp}) and a plastic portion (J_{pl}^{ccp}), that is, $J^{ccp} = J_{el}^{ccp} + J_{pl}^{ccp}$.

(2) The plastic zone size correction (or small scale yielding correction) is applied to J_{el}^{ccp} (Kumar and Shih, 1980).

(3) The CCP plate solution is corrected for the curvature of the shell or cylindrical structure. The approximated J-integral values for the tank shell (J_{el}^{cur} and J_{pl}^{cur}) are
$J_{el}^{cur} = Y^2\ J_{el}^{ccp}$ and $J_{pl}^{cur} = Y^2\ J_{pl}^{ccp}$, respectively.

(4) The contributions of fracture parameters from the other sources, such as thermal stress or residual stress, can be combined in the sense of linear elastic fracture mechanics. The elastic portion of J-integral (J_{el}^{cur}) in (4) above is first converted to K_I^{appl} , the Mode I stress intensity factor due to applied load:
$K_I^{appl} = \sqrt{E\ J_{el}^{cur}}$, for the plane stress condition.

(5) A residual stress contribution can be included in the J-integral solution using the formula advanced by Green and Knowles (1994). The residual stress distribution is a self-equilibrium, symmetric pattern with maximum tension ($+\sigma_r$) on the edges and maximum compression ($-\sigma_r$) in the mid-section of the plate. The through-thickness variation from tension-compression-tension is assumed to be a cosine shape. The σ_r value is taken to be the yield stress of the base metal. The maximum stress intensity factor is $K_{max}^{res} = 0.43\sigma_r\sqrt{\pi t}$. Note that K_I^{res} is saturated to a maximum value when the crack is extended in length only a fraction of the plate thickness. Therefore, the residual stress of this type is not subject to curvature correction.

(6) The total elastic portion of J is calculated as $J_{el} = \frac{1}{E}\left(K_I^{appl} + K_{max}^{res}\right)^2$.

(7) The plastic portion of J remains unchanged, that is, $J_{pl} = J_{pl}^{cur}$.

(8) Finally, the total J-integral of the crack is $J = J_{el} + J_{pl}$.

Based on the calculation procedure described above, the instability crack length as a function of applied stress is shown in Figure 5, for an example tank with radius 510 inches (12.95 m), height 320 inches (8.13 m), and wall thickness 5/8 inches (15.875 mm). The remote applied stress is perpendicular to the crack and is up to the yield stress of the material (256 MPa or 37.1 ksi). Both solutions for an axial crack (2b is the height of the storage tank) and for a circumferential crack (2b is the circumference of the storage tank) are presented.

Finite Element Analysis of an Arbitrary Flaw in a Storage Tank

As a demonstration of the J-Integral fracture methodology applied to a flaw in a tank and to validate the application of the CCP solution to the tank configuration, a finite element analysis was performed for an arbitrary flaw in storage tank geometry. This flaw has an arc length of about 16 inches or 406 mm (the projection length is about 13 inches or 330 mm perpendicular to the direction of the applied stress).

The finite element region was chosen such that the flaw is away from the edges of the model to minimize the boundary effects. The mesh shown in Figure 6 was generated with MSC/PATRAN (1996), a finite element analysis pre/post-processor. The near crack tip elements were refined for accurately evaluating the J-integral. In addition, it was designed for a potential crack extension analysis for the right-end crack tip.

This finite element model contains 2096 four-noded plane stress elements with 2192 nodes before the multi-point constraints are applied (for example, for zipping the nodes ahead of the crack tip in the direction of crack growth). The true stress-true strain curve is characterized by the Ramberg-Osgood power law. The mechanical properties for input to the finite element program are: Young's modulus 208 GPa (30,000 ksi), Poisson's ratio 0.333, yield stress 256 MPa (37.1 ksi), and the Ramberg-Osgood parameters α and n, respectively, 17.176 and 3.585 (Fig. 4).

The ABAQUS finite element program (1998) was used for the analysis. For a radius to thickness ratio that is extremely large (> 800), the curvature effect of the tank is insignificant and the plane stress elements can be used for calculation. The J-integral values were obtained at each load level up to the yield stress (256 MPa or 37.1 ksi) as shown in Figure 7. It can be seen that the cut-off J (450 kJ/m^2 or 2570 in-lb/in^2) corresponds to an applied stress level equal to 58% of the yield stress, or 150 MPa (22 ksi). This stress level is equivalent to an instability flaw size about 10-inch (254 mm) long according to

Figure 5 which was based on CCP solution. This demonstrates that the curvature-corrected CCP solution is a close approximation of J-integral for a complex flaw in storage tanks. Furthermore, it provides a methodology for assessing the fitness-for-service of storage tanks for known loading conditions and safety margins.

Maximum Tank Fluid Level Based on Flaw Stability

The J-T flaw stability methodology can be used to determine the maximum fluid level in a storage tank with a postulated flaw. For demonstration purpose, the applied stress is assumed to be caused only by the hydrostatic pressure of the fluid in the tank. The maximum hoop stress is, therefore, $\rho ghR/t$, where ρ is the density of the fluid, g is the gravitational constant, h is the height of the fluid in the tank, R is the radius of the tank, and t is the tank wall thickness. Using a cut-off J-integral value (450 kJ/m^2 or 2570 in-lb/in^2), the corresponding instability crack length can be calculated for various fluid densities of the contents in the tank. A family of curves, each curve corresponding to a particular fluid density, can be plotted for fluid level versus instability crack length. By cross plotting, Figure 8 is obtained. This figure indicates the maximum height of the fluid that can be filled in the tank before a certain size of flaw becomes unstable. For any field data point (fill level for certain kind of fluid) located below a curve with a specified crack size, the tank can be operated without causing sudden rupture due to the existence of this flaw which is located in the highest stress area of the tank. Of course, the applied stress is not limited to the hydrostatic pressure of the tank contents. It may include stresses from other sources such as the thermal gradient, pump operation, and seismic excitation, etc. The crack in the tank may be a postulated flaw for a structural integrity assessment. Safety factors can be included in the analysis.

Conclusion

An elastic-plastic fracture methodology based on J-integral was used to investigate the flaw stability in mild steel storage tanks. Finite element analysis of an arbitrary flaw in a tank showed that the analytical solution for a center-cracked panel with curvature correction is a close approximation. Because the material and the applied J-T curves do not intersect unless by extrapolation, a conservative cut-off J value corresponding to 1.5-mm (0.06-inch) stable crack growth was used to define the instability crack length. The resulting relationship between the instability flaw size and the applied stress can be used to provide guidelines for assessing the fitness-for-service of existing storage tanks for known loading conditions and safety margins. The maximum fluid level for the contents of the storage tank can be established based on a postulated flaw size in the tank. The postulated size should bound any existing flaw sizes.

Acknowledgment

The authors acknowledge the many helpful discussions with our colleague Dr. B. J. Wiersma. This work was supported by the U. S. Department of Energy under contract No. DE-AC09-96SR18500.

References

ABAQUS/STANDARD, Version 5.7, Hibbitt, Karlsson & Sorensen, Inc., Pawtucket, Rhode Island, 1998.

Green, D. and Knowles, J., "The Treatment of Residual Stress in Fracture Assessment of Pressure Vessels," Journal of Pressure Vessels Technology, Vol. 116, pp. 345-352, 1994.

Hutchinson, J. W. and Paris, P. C., "Stability Analysis of J-Controlled Crack Growth," Elastic-Plastic Fracture, ASTM Special Technical Publication 668, pp. 37-64, 1979.

Kumar, V. and Shih, C. F., "Fully Plastic Crack Solutions, Estimation Scheme, and Stability Analyses for the Compact Specimen," Fracture Mechanics: Twelfth Conference, ASTM STP 700, American Society for Testing and Materials, 1980, pp. 406-438.

Lam, P. S., Sindelar, R. L., and Awadalla, N.G., "Acceptance Criteria for In-service Inspection of Heat Exchanger Head and Shell Components," in Fatigue and Fracture of Aerospace Structural Materials, ed. A. Nagar and A.-Y. Kuo, American Society of Mechanical Engineers, AD-Vol. 36, pp. 43-57, 1993.

MSC/PATRAN, Version 7.5, MacNeal-Schwendler Corporation, Los Angeles, California, 1996.

Shih, C.F. and Hutchinson, J.W., "Fully Plastic Solutions and Large Scale Yielding Estimates for Plane Stress Crack Problems," Trans. American Society of Mechanical Engineers, Journal of Engineering Materials and Technology, Series H, Vol. 98, pp. 289-295, 1976.

Sindelar, R. L., Lam, P. S., Caskey, G. R. Jr., and Woo, L. Y. "Flaw Stability in Mild Steel Tanks in the Upper-Shelf Ductile Range – Part I: Mechanical Properties," to be published in ASME Journal of Pressure Vessel and Technology, 1999.

Tada, H., Paris, P.C. and Irwin, G.R., The Stress Analysis of Cracks Handbook, Second Edition, pages 33.3, 33.4, 33.6 and 34.1, Paris Productions Incorporated (and Del Research Corporation), Saint Louis, MO, 1985.

Figure Captions

Figure 1 J-T methodology for instability crack length

Figure 2 Lower bound J_R curve for A285 carbon steel piping material

Figure 3 Crack extension limit of valid J-deformation for a 0.394T C(T) planform specimen

Figure 4 Ramberg-Osgood fit for a lower bound A285 specimen

Figure 5 Instability crack length for a mild steel storage tank

Figure 6 Finite element mesh for an arbitrary crack

Figure 7 J-integral solution for an arbitrary crack

Figure 8 Maximum fluid level in storage tank with a postulated crack

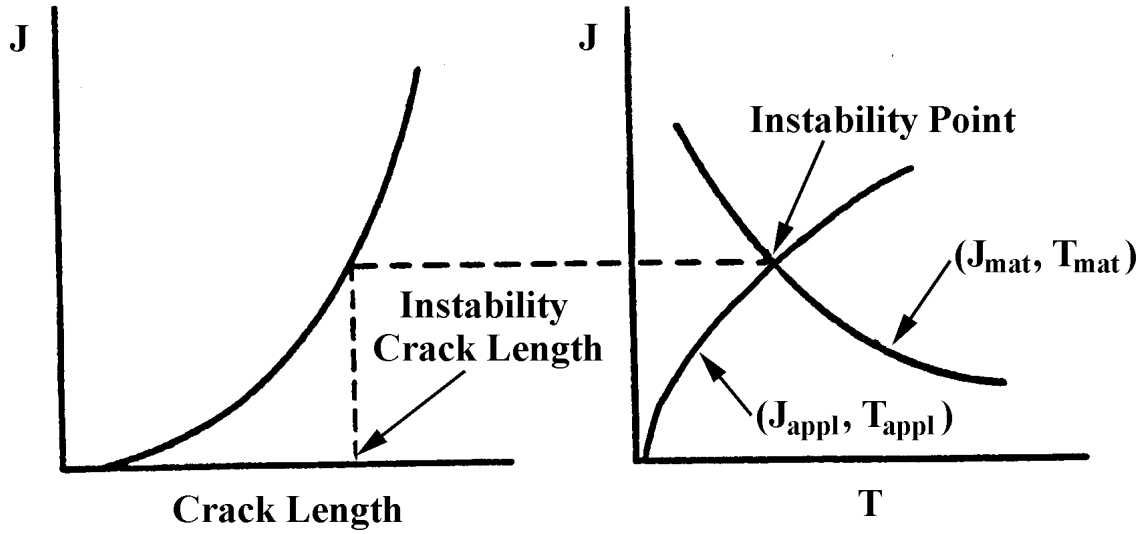

Figure 1 J-T methodology for instability crack length

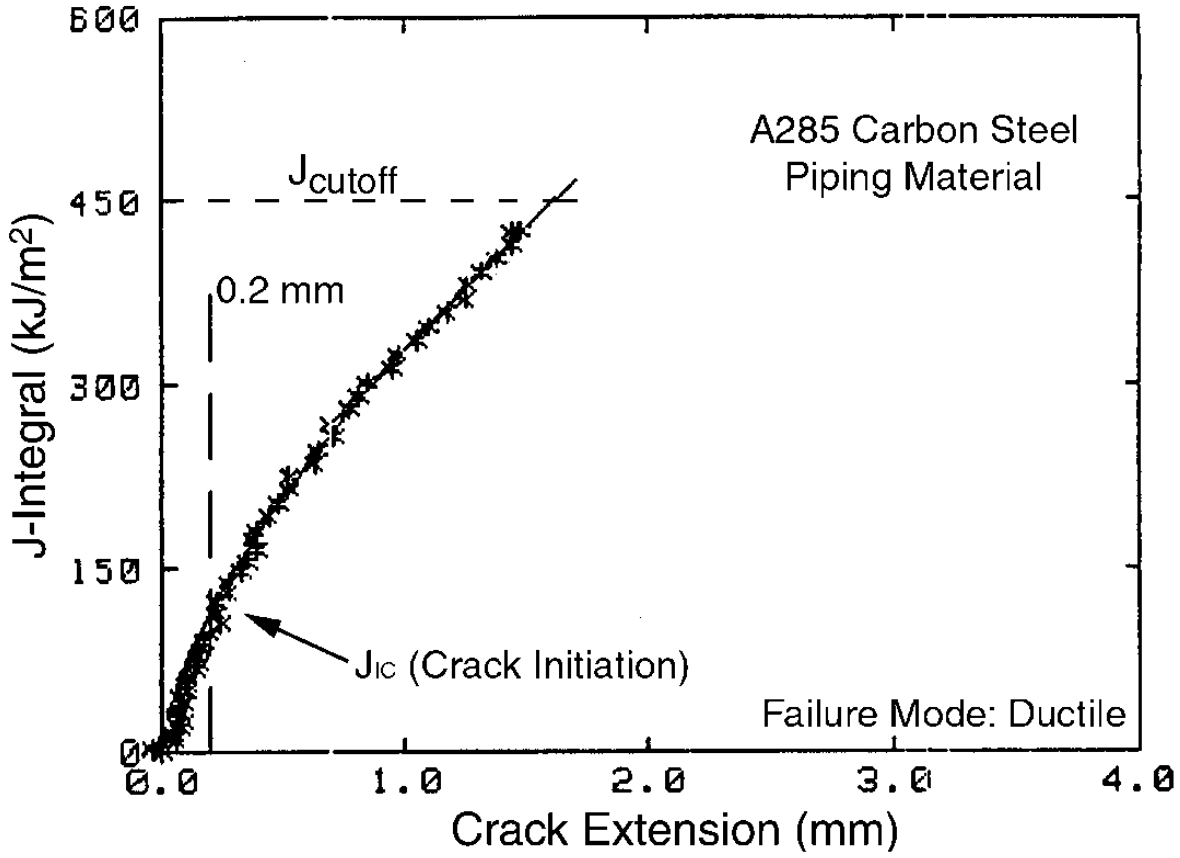

Figure 2 Lower bound J_R curve for A285 carbon steel piping material

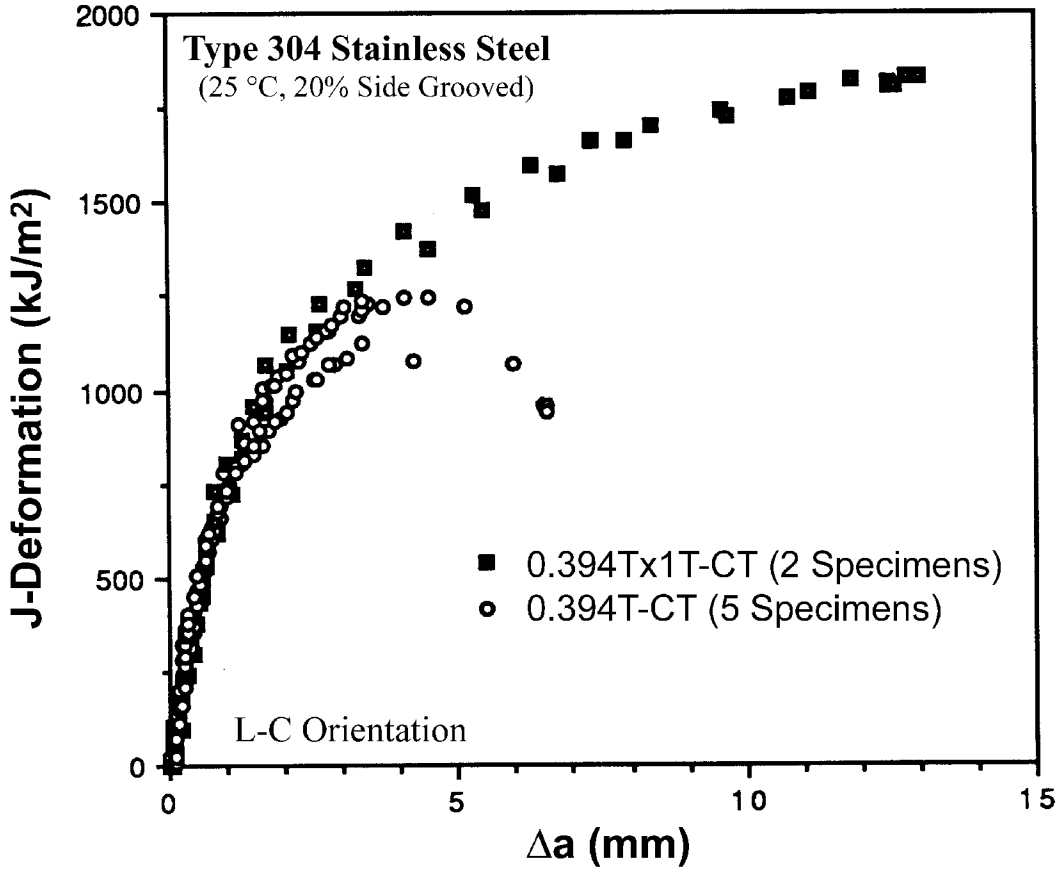

Figure 3 Crack extension limit of valid J-deformation for a 0.394T C(T) planform specimen

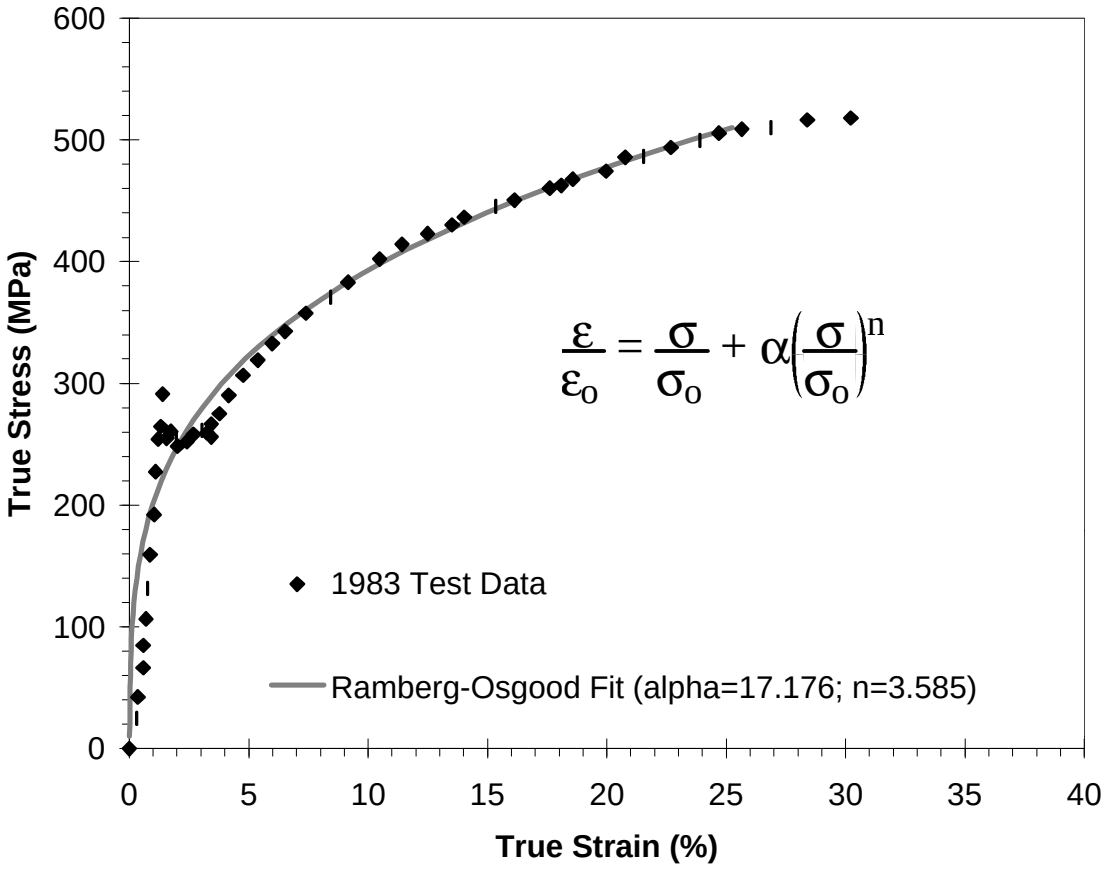

Figure 4 Ramberg-Osgood fit for a lower bound A285 specimen

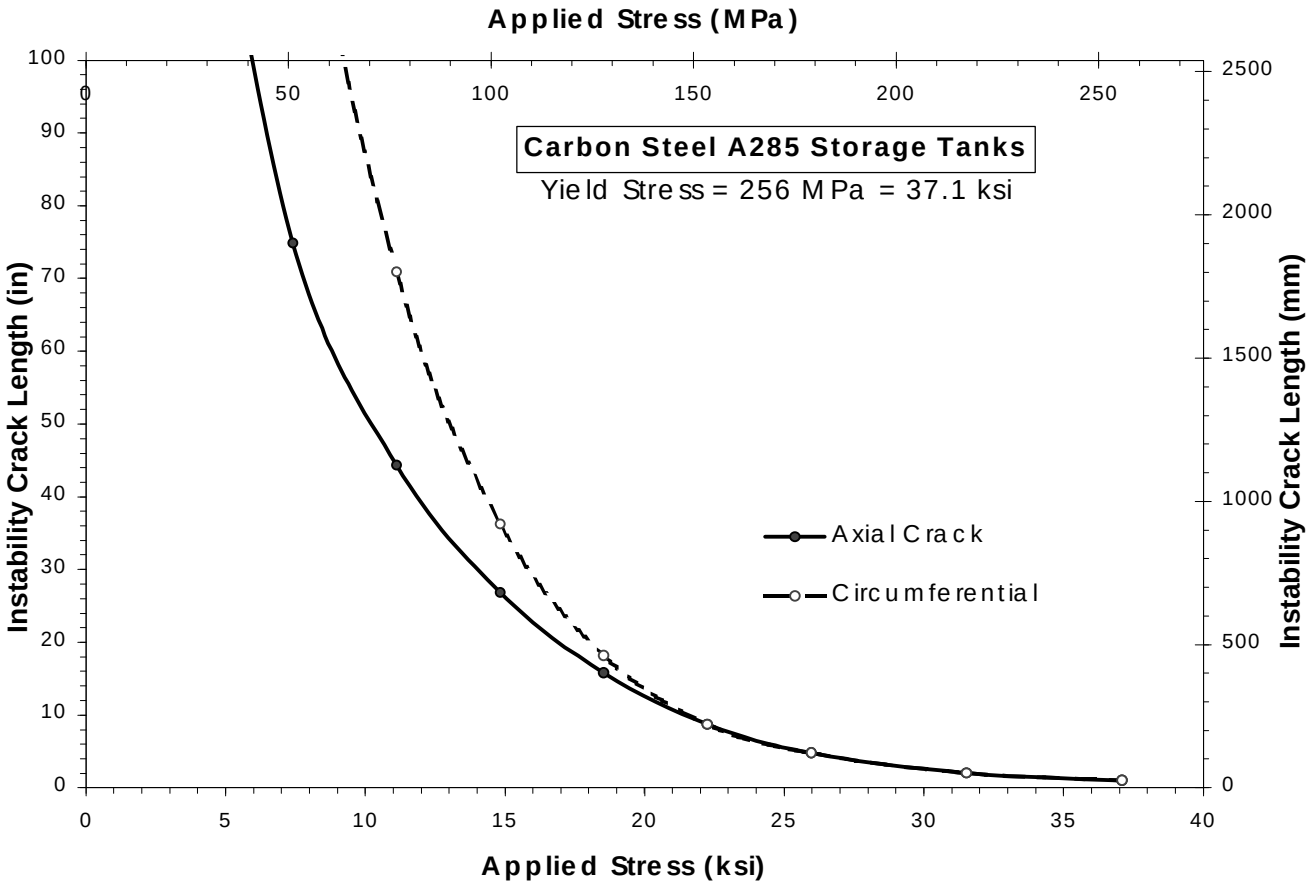

Figure 5 Instability crack length for a mild steel storage tank

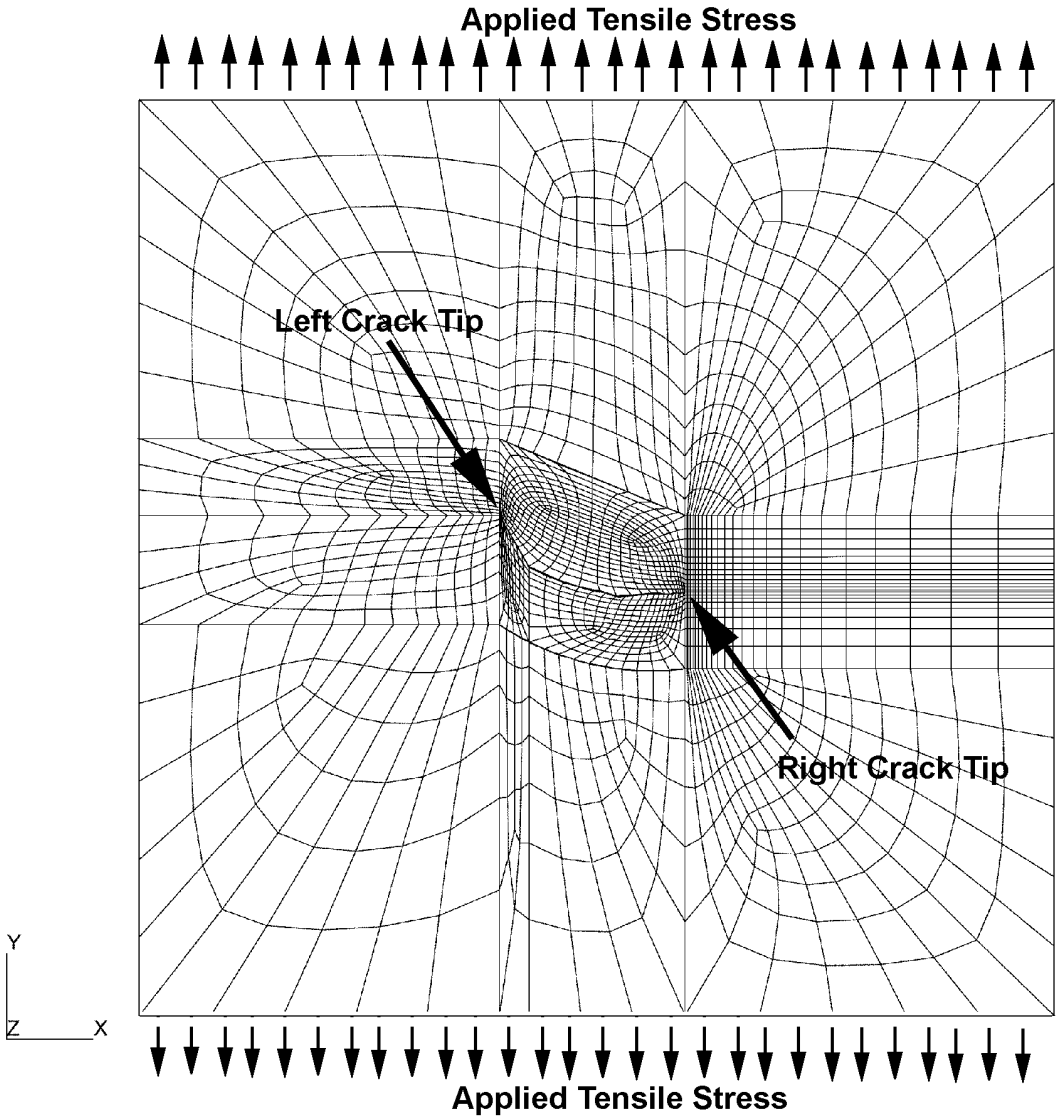

Figure 6 Finite element mesh for an arbitrary crack

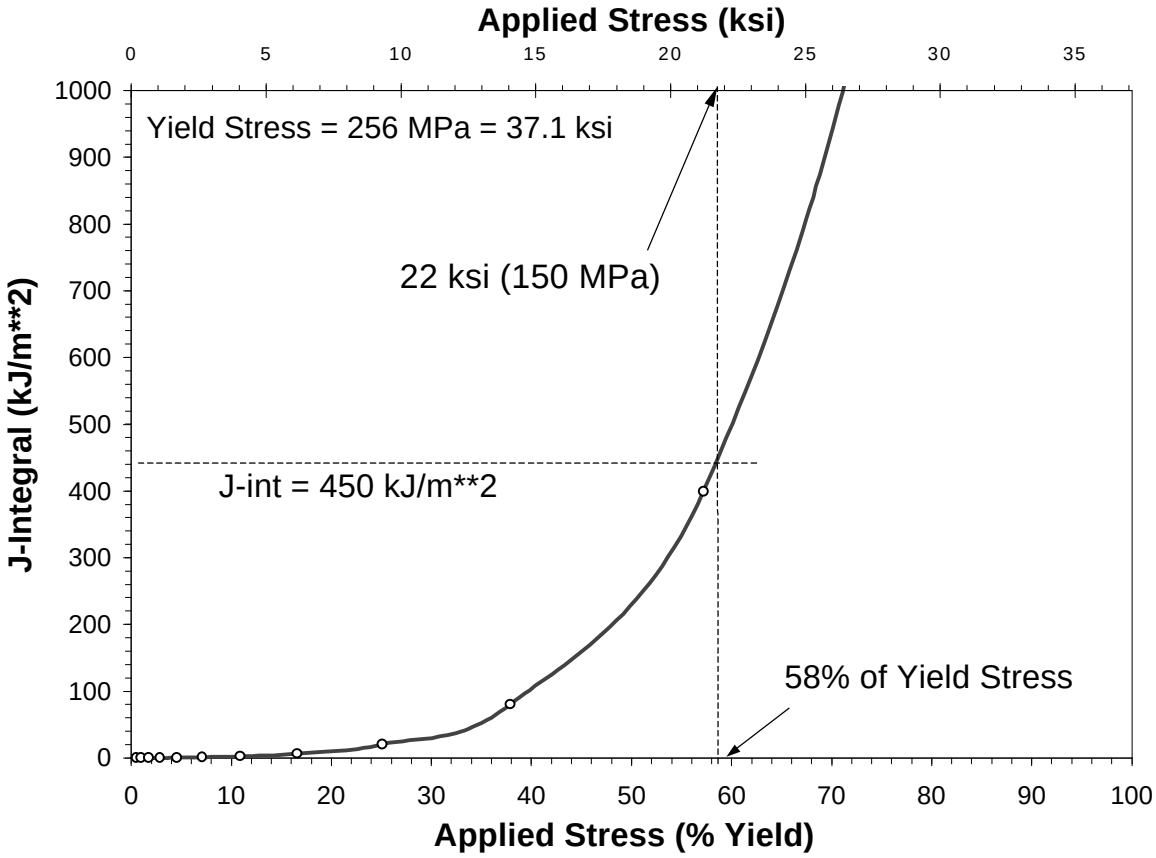

Figure 7 J-integral solution for an arbitrary crack

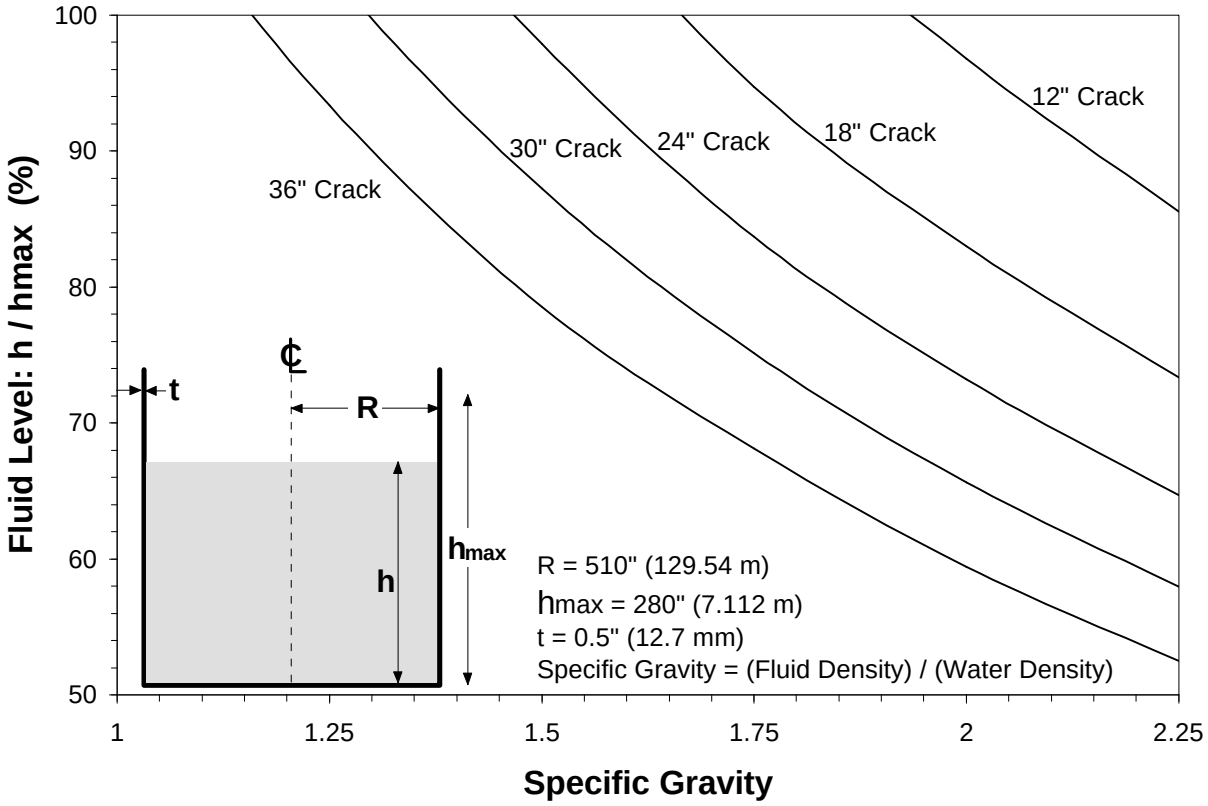

Figure 8 Maximum fluid level in storage tank with a postulated crack